

Article

Diastereomeric Effect on the Homolysis of the C–ON Bond in Alkoxyamines: A DFT Investigation of 1,3-Diphenylbutyl-TEMPO

Alexandra Blachon, Sylvain R. A. Marque *, Val érie Roubaud and Didier Siri

UMR 6264 LCP CNRS-Aix-Marseille Université case 521, Avenue Escadrille Normandie-Niemen, 13397 Marseille Cedex 20 France; E-Mails: familleblachon@cegetel.net (A.B); val érie.roubaud@univ-provence.fr (V.R.), didier.siri@univ-provence.fr (D.S.)

* Author to whom correspondence should be addressed; E-Mail: sylvain.marque@univ-provence.fr.

Received: 2 September 2010; in revised form: 16 September 2010 / Accepted: 16 September 2010 / Published: 27 September 2010

Abstract: The rate constants k_d of the homolysis of the C–ON bond in styryl dyads TEMPO-based alkoxyamines have recently been published (Li *et al. Macromolecules* **2006**, *39*, 9201). The diastereoisomers exhibited different values which were higher than for the unimer TEMPO-styryl alkoxyamine **1**. At a first glance, the localization of the steric strain was not obvious. To decipher this problem, diastereoisomer models **2** (*RR/SS*) and **3** (*RS/SR*), as well as the released alkyl radicals, were calculated at the B3LYP/6-31G(d) level. It was revealed that the increase in k_d from **1** to **3** was due to the compression (buttressing effect) of the reactive center by the second styryl moiety. The difference in k_d for the diastereoisomer was clearly an activation entropy effect ΔS^\ddagger because the alkyl fragment of the *RS/SR* diastereoisomer exhibited the same conformation as the released radical whereas the conformation for the *RR/SS* diastereoisomer was quite different and thus required the rotation of several bonds to reach the correct TS, which cost ΔS^\ddagger , and thus lowers k_d .

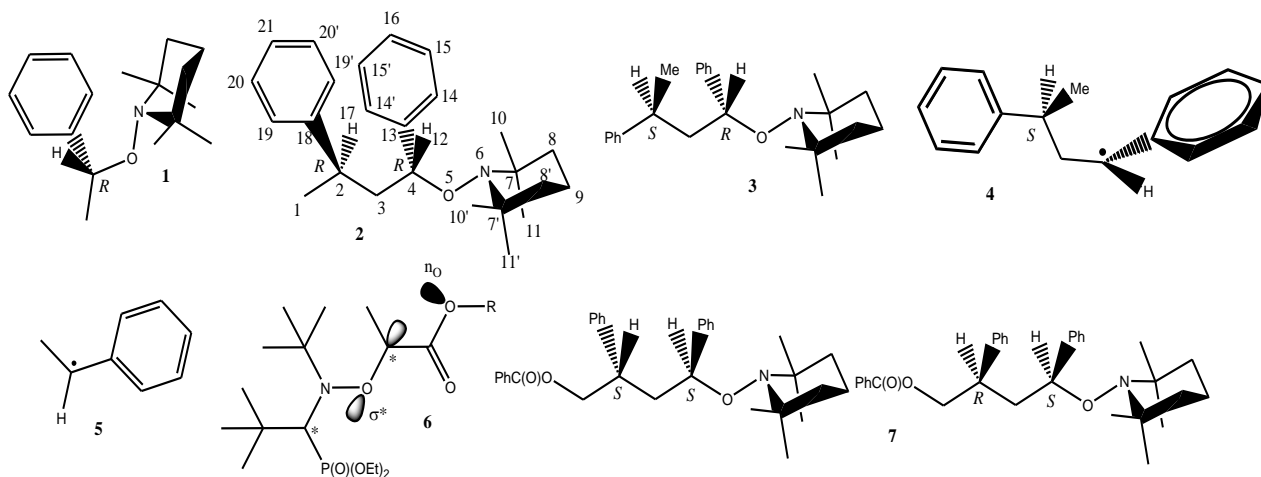
Keywords: DFT calculations; nitroxide mediated polymerization; remote steric effect

1. Introduction

Since the pioneering work of Rizzardo in 1985 [1], research progress in Nitroxide Mediated Polymerization (NMP) has undergone exponential growth in the areas of materials preparation [2], kinetic investigations [3–5], and in the design of new initiators/controllers [6,7]. It has been shown that each stage—initiation, propagation, and termination—of the polymerization is important for the fate of NMP [8,9]. Over the last two decades, a tremendous amount of work has focused on analyzing the effects ruling the homolysis of the C–ON bond of the initiator/controller. The accumulation of data has shown that understanding the effects occurring during the C–ON bond homolysis is crucial for the design of new initiators. During the last decade, the effect of the penultimate unit on the C–ON bond was poorly investigated, and seemingly contradictory results were published concerning polystyryl-TEMPO alkoxyamines. Until recently, it has been shown [10] that the penultimate unit may exert a dramatic effect on the C–ON bond homolysis and, consequently, on the fate of NMP [11,12]. Georges and colleagues [13] measured the C–ON bond homolysis in the diastereoisomers of styryl dyads of TEMPO-based alkoxyamines **7** (Figure 1). They reported that the (*S,S*) diastereoisomer [14] was cleaving two-folds as slowly as the (*R,S*) diastereoisomers. However, no ambiguous discussions were provided on the origin of this effect. At a first glance, although this led to apparently contradictory measurements [10,15,16], such small differences in k_d may look unimportant, but nevertheless, we have recently shown that the fate of NMP [11,12,17] and the occurrence of side-reactions [18] depends on such small differences.

A few years ago, we showed that the two-fold difference between the two diastereoisomers of 1-alkoxycarbonyl ethyl based-SG1 **6** was due to the hyperconjugative effect ($n_{\text{OCO}} \rightarrow \sigma^*_{\text{C-ON}}$ interaction) between the carbonyloxyl group and the C–ON bond (Figure 1) [19]. Then, for the homolysis **1–5** (Figure 1), we show hereafter that hyperconjugative interactions play a minor role, in sharp contrast with the remote steric effect.

Figure 1. Molecules investigated.

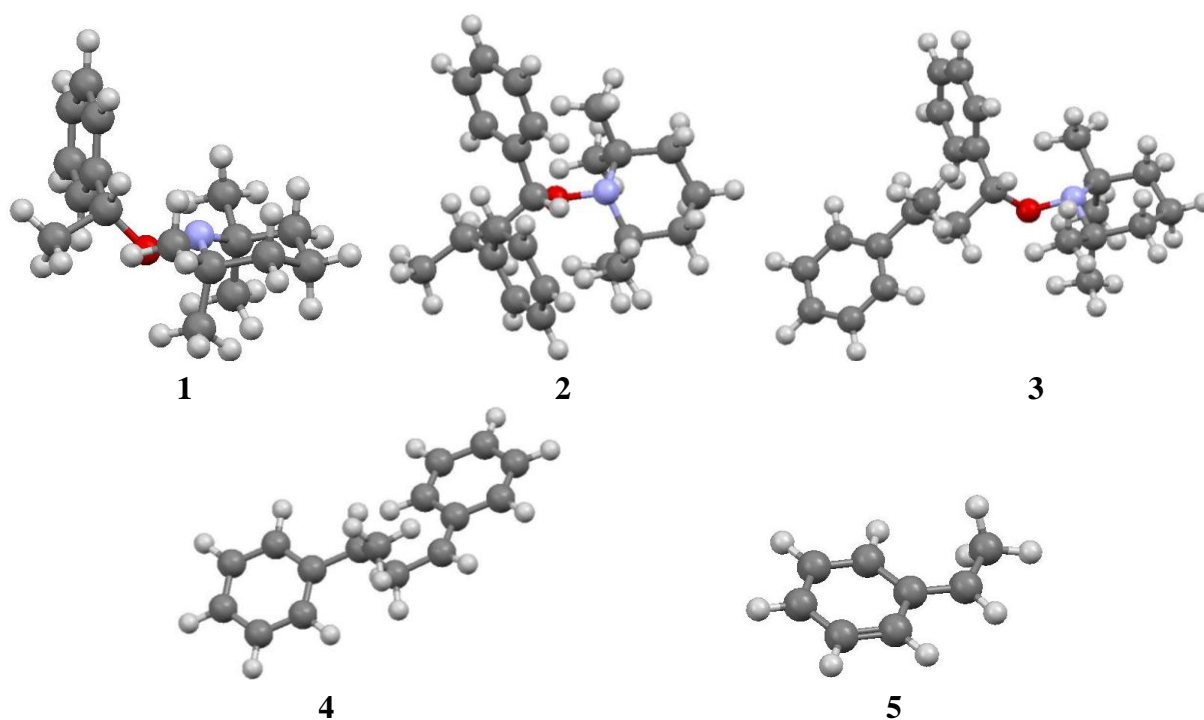


2. Computational Method

In recent articles [19,20], we investigated the hyperconjugation effect as well as the steric strain [21] using Density Functional Theory (DFT) calculations at the B3LYP/6-31G(d) level of

theory. All calculations were performed using the Gaussian 03 molecular orbital package [22]. Geometry optimizations were carried out without constraints (Figure 2) [23,24]. Vibrational frequencies were calculated at the B3LYP/6-31G(d) level to determine the nature of the located stationary points. Frequency calculations were performed to confirm that the geometry was a minimum (zero imaginary frequency). The single point energies were then calculated at the B3P86/6-311++G(d,p) level of theory for molecules 1–5 [25]. Radical Stabilization Energies (RSE) of 4 and 5 were calculated at G3B3MP2 (compound method). For 1–3, Natural Bond Orbital (NBO) analysis [19,26] was performed with the NBO 3.1 program in the Gaussian 03 package. For NBO analysis on 4 and 5, more details are provided as Supplementary information.

Figure 2. DFT calculated structures for molecules 1–5.



3. Results and Discussion

Georges and colleagues [13] reported different homolysis rate constants k_d at 120 °C for the *RR/SS* ($k_d = 9.7 \times 10^{-4} \text{ s}^{-1}$) and *RS/SR* ($k_d = 19.6 \times 10^{-4} \text{ s}^{-1}$) diastereoisomers of **7** (Figure 1) as well as for the unimeric species **1** ($k_d = 5.5 \times 10^{-4} \text{ s}^{-1}$). It is known [19,27,28] that the steric effect ruling the C–ON bond homolysis is related to the geometrical parameters—bond length l , interatomic distance d , valence angle α , and torsion angle θ —of the alkoxyamines. However, as the diastereoisomers of **7** are large molecules (71 atoms) implying time consuming calculations, it was assumed that the benzyloxy group exhibited neither significant polar effect nor important steric effect and that the second styryl group did not exhibit significant polar effect [10]. Hence, DFT calculations were performed on smaller (58 atoms) molecule models 1–4 (Figure 2 and Table 1) to investigate the effect of the penultimate units of 2–4 as well as the effect of their configurations and conformations. Interestingly, the bond lengths O₅–C₄, N₆–O₅, C₄–C₁₃, C₃–C₄, the distance C₄ ••N₆, the valence angles $\langle \text{N}_6\text{O}_5\text{C}_4 \rangle$, $\langle \text{C}_3\text{C}_4\text{O}_5 \rangle$, $\langle \text{C}_{13}\text{C}_4\text{O}_5 \rangle$, and the torsion angles $\langle \text{C}_4\text{O}_5\text{N}_6\sigma_{\text{N}_6} \rangle$, $\langle \text{N}_6\text{O}_5\text{C}_4\text{H}_{12} \rangle$, $\langle \text{O}_5\text{N}_6\text{C}_7\text{C}_{11} \rangle$ did not differ

markedly among **1**, **2**, and **3**. This means that no peculiar steric strains were observed except that the phenyl ring was tilted ($\langle O_5C_4C_{13}C_{14} \rangle$) from 4° to 6° closer from 90° from unimolecular alkoxyamine **1** to dimeric alkoxyamines **2** and **3**, involving possible $\pi \rightarrow \sigma^*_{O_5-C_4}$ interaction (Figure 3d). Thus, all the molecules exhibited the same conformation around the reactive center, that is, the alkyl group and H_{12} almost eclipsed the nitrogen lone pair, and the C_4-C_{13} bond was almost perpendicular to the $N-O$ bond (Figure 3a–c).

Figure 3. Newman projections given by the torsion angles θ gathered in Table 1.

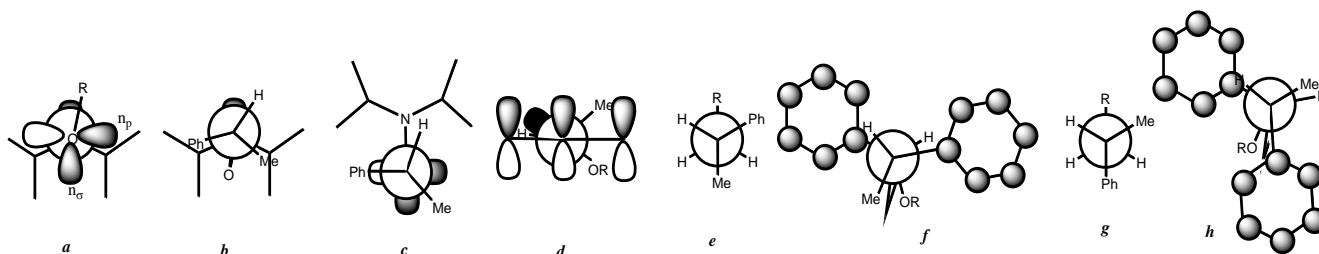


Table 1. Geometrical parameters (bond length l , interatomic distance d , valence angle α and torsion angle θ), interaction energy, and formation enthalpy ΔH_f calculated by DFT at the B3LYP/6-31G(d) level of theory.^a

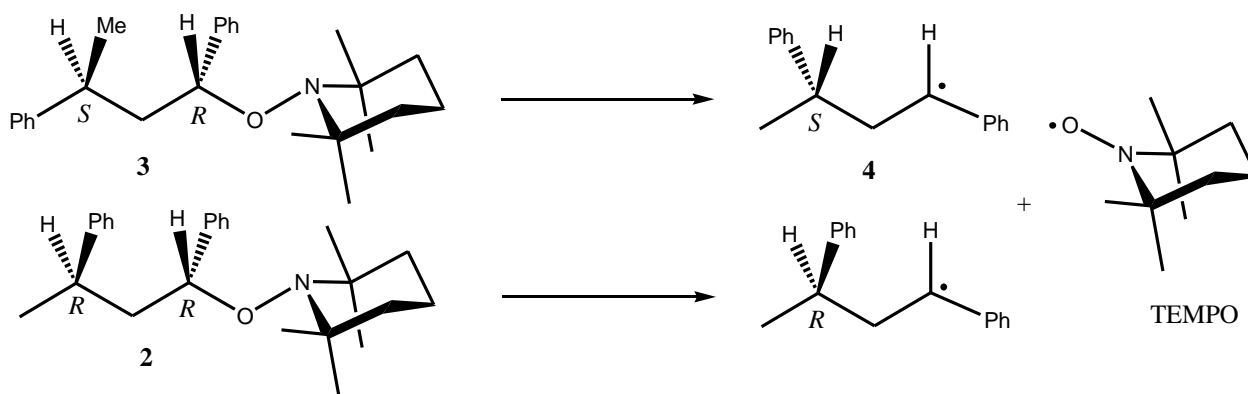
l (Å)	1 (X-ray)	1 (R)	2 (R ₁ R ₂)	3 (R ₁ S ₂)	4 (S ₂)	5
O ₅ –C ₄	1.452	1.447	1.450	1.449	–	–
N ₆ –O ₅	1.458	1.453	1.453	1.453	–	–
C ₄ –C ₁₃	1.505	1.521	1.521	1.520	1.416	1.416
C ₃ –C ₄	1.521	1.533	1.539	1.541	1.498	1.497
C ₂ –C ₃	–	–	1.546	1.547	1.566	–
d (Å)						
C ₄ ⋯ N ₆	2.420	2.427	2.432	2.430	–	–
H ₁₂ ⋯ C ₁₀	2.707	2.708	2.637	2.686	–	–
C ₁₃ ⋯ C ₃	2.509	2.508	2.540	2.536	2.594	2.582
H ₁₂ ⋯ C _{18/1}	–	–	2.862	2.886	3.184	–
C ₁₃ ⋯ H ₁₇	–	–	2.706	2.699	3.200	–
H ₁₂ ⋯ H ₁₇	–	–	3.183	3.197	3.508	–
C ₁₃ ⋯ C ₂	–	–	3.100	3.097	3.461	–
C ₂ ⋯ C ₄	–	–	2.611	2.618	2.573	–
α (°)						
$\langle N_6O_5C_4 \rangle$	112.5	113.7	113.9	113.7	–	–
$\langle C_3C_4O_5 \rangle$	105.0	106.1	104.7	104.9	–	–
$\langle C_{13}C_4O_5 \rangle$	112.3	113.5	113.7	113.1	–	–
θ (°)						
$\langle O_5C_4C_{13}C_{14} \rangle$	61.6	54.6	60.3	58.5	–	–
$\langle C_4O_5N_6\sigma_{N_6} \rangle^b$	–12.0	–13.7	–15.4	–14.0	–	–
$\langle N_6O_5C_4H_{12} \rangle$	–29.6	–23.5	–28.2	–25.2	–	–
$\langle O_5N_6C_7C_{11} \rangle$	50.3	49.8	50.0	50.4	–	–
$\langle C_{19}C_{18}C_2C_3 \rangle$	–	–	–61.0	67.5	67.0	–
$\langle C_1C_2C_3C_4 \rangle$	–	–	172.7	–62.8	60.6	–
$\langle C_2C_3C_4C_{13} \rangle$	–	–	–58.2	–58.2	86.5	–

Table 1. Cont.

l (Å)	1 (X-ray)	1(R)	2(R4R2)	3(R4S2)	4(S2)	5
Interaction energies (kJ/mol)						
$\pi_{\beta,C18} \rightarrow \sigma^*_{\beta,C3-C4}$	—	—	—	—	6.0	—
$\sigma_{\beta,C3-C4} \rightarrow \beta\text{-LUMO}$	—	—	—	—	11.0	14.0 ^c
$\alpha\text{-SOMO} \rightarrow \sigma^*_{\alpha,C3-C4}$	—	—	—	—	22.0	15.0 ^d
$\sigma_{\alpha,C3-C4} \rightarrow \pi^*_{\alpha,C18}$	—	—	—	—	5.0	—
$\alpha\text{-SOMO} \rightarrow \pi^*_{\alpha,C13}$	—	—	—	—	165.0	162.0
$n_{\sigma,O} \rightarrow \sigma^*_{C3-C4}$	—	0.0 ^e	2.0	2.0	—	—
$\sigma_{C3-C4} \rightarrow \pi^*_{C18}$	—	—	7.0	9.0	—	—
$\pi_{C13} \rightarrow \sigma^*_{C-O}$	—	19.0	22.0	21.0	—	—
ΔH_f (kJ/mol)	—	—	—	-3.0 ^f	—	—

^a Dash is for "not determined"; ^b $\langle C_4O_5N_6\sigma_{N6} \rangle = \langle C_4O_5N_6C_{10/10} \rangle - 120$ °; ^c The donation was from the bonding spin-orbital β C–H to the β -LUMO. The conformation implied the donation from a second H atom of the methyl group; ^d The donation was from the α -SOMO to the antibonding spin-orbital α C–H of the methyl group. The conformation implied the donation from a second H atom; ^e No $n_{\sigma,O} \rightarrow \sigma^*_{C3-C4}$ interaction was observed for **5**. ^f $\Delta H_f = H_f(\mathbf{3}) - H_f(\mathbf{2})$.

Importantly, the homolysis of diastereoisomers **2** and **3** afforded either the same alkyl radical or its enantiomeric pair **4** (Scheme 1).

Scheme 1. Homolysis of diastereoisomers of alkoxyamines **2** and **3**.

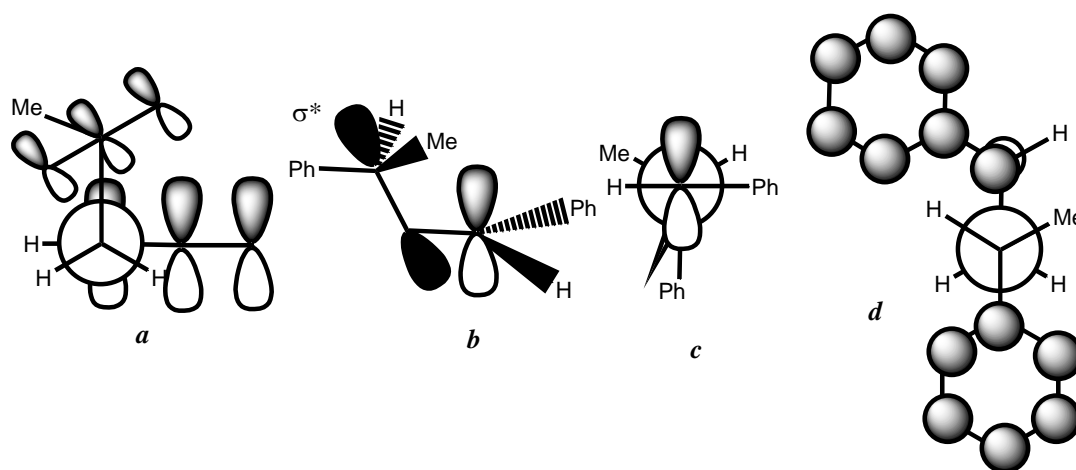
As no differences in the geometrical parameters were observed at the reaction center N–O–C, the RSE of the released **4** and **5** radicals were calculated using the isodesmic reaction (1).



Thus, RSE were estimated to be 56.0 kJ/mol and 61.0 kJ/mol for **4** and **5**, respectively, implying that **5** was 5.0 kJ/mol more stabilized than **4**, despite the $\pi_{\beta,C18} \rightarrow \sigma^*_{\beta,C2-C3} / \sigma_{\beta,C2-C3} \rightarrow \beta\text{-LUMO}$ and $\alpha\text{-SOMO} \rightarrow \sigma^*_{\alpha,C2-C3} / \sigma_{\alpha,C2-C3} \rightarrow \pi^*_{\alpha,C18}$ interactions (Table 1). Indeed, **4** and **5** exhibited strong $\alpha\text{-SOMO} \rightarrow \pi^*_{\alpha,C13}$ interactions, as highlighted by the *ca.* 0.1 Å shortening of the C₄–C₁₃ bonds, and weak $\alpha\text{-SOMO} \rightarrow \sigma^*_{\alpha,C3-C4}$ and $\alpha\text{-SOMO} \rightarrow \sigma^*_{\alpha,C-H}$ interactions for **4** and **5**, respectively, as highlighted by the *ca.* 0.05 Å shortening of the corresponding bonds as well as the shortening of the C₂–C₄ distance. Interestingly, weak but significant $\pi_{\beta,C18} \rightarrow \sigma^*_{\beta,C2-C3}$ and $\sigma_{\alpha,C2-C3} \rightarrow \pi^*_{\alpha,C18}$ interactions

avored the *anti* conformation around the C₁–C₃ bond ($\langle C_1C_2C_3C_4 \rangle = 60^\circ$; Figure 4d) and the perpendicular arrangement between the C₁₃—aromatic ring and the C₂–C₃ bond ($\langle C_2C_3C_4C_{13} \rangle = 86.5^\circ$; Figure 4d). The weakness of these interactions was partly due to the tilted position ($\langle C_{19}C_{18}C_2C_3 \rangle = 23^\circ$; Figure 4a) of the aromatic ring relative to the C₂–C₃ bond (Table 1, Figure 4). It is noteworthy that the relief of the steric strain is more important from **2/3** to **4** ($\Delta d_{C_{13}\cdots C_2} = 0.36 \text{ \AA}$) than from **1** to **5** ($\Delta d_{C_{13}\cdots H} = 0.23 \text{ \AA}$). However, **4** was still more constrained than **5**, as highlighted by the smaller variation of $d_{C_{13}\cdots C_3}$ for **5** than for **4** (0.05 Å and 0.08 Å, respectively) which means that **4** was less stabilized than **5**. The stabilization and the interactions discussed above cannot account for the reported reactivity, *i.e.*, k_d for **3** and **4** larger than k_d for **1**. As the homolysis is an endothermic reaction, the structure of TS was expected to resemble the structure of the products, that is, radicals **4** and **5**, and TEMPO. As TEMPO was always released, any changes observed were due to the structure/configuration/conformation of the alkyl fragments and radicals. As mentioned above, some Δd values pointed to a relief of steric strain in **3** and **4**, leading to an increase in the freedom of motion at TS, and thus in ΔS^\ddagger , and also in k_d of **3** and **4**. This was highlighted by the 0.3 Å–0.5 Å increase in the distances H₁₂ ···C_{18/1}, C₁₃ ···C₂, C₁₃ ···H₁₇, and H₁₂ ···H₁₇ from alkoxyamines **2/3** to radicals **4**.

Figure 4. Newman's projections for various conformations for the alkyl radical: (a) along the C3–C4 bond; (b) $\sigma^*_{C-C} \rightarrow$ SOMO interaction; (c) along the C4 ···C2 axis; (d) along the C3–C2 bond.

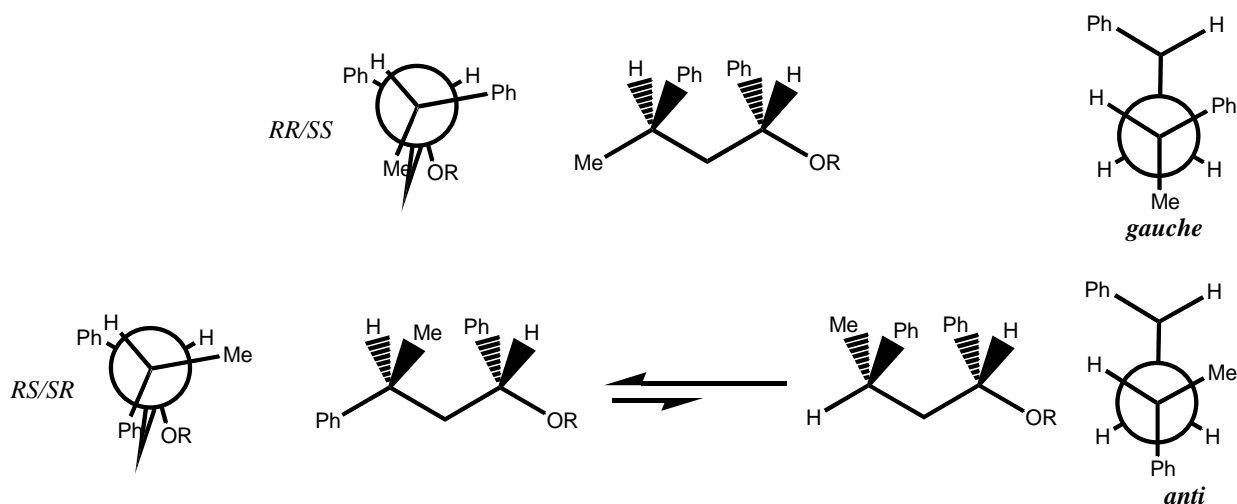


As mentioned above, the homolysis of **1–3** was an endothermic reaction, which means that their TS resembled the products (TEMPO and the alkyl radicals) [29]. For the alkyl radicals, it is noteworthy to mention that the odd electron was delocalized on the aromatic ring by conjugation of the SOMO and the π cloud, which implied a 90° angle between the aromatic ring and the SOMO (α -SOMO $\rightarrow \pi^*_{\alpha, C_{13}}$), and consequently, at TS, aiming to favor this interaction, it is expected that the cleaving O–C bond, *i.e.*, the nascent SOMO, exhibited an angle $\langle O_5C_4C_{13}C_{14} \rangle$ as close as possible from 90° . Hence, this remote internal strain implied a 4° – 6° opening of the torsion angle $\langle O_5C_4C_{13}C_{14} \rangle$ for **2** and **3** in comparison to **1**, forcing the aromatic ring to stand in a better position and reducing entropic cost at TS, as well as slightly improving (3 kJ/mol more) the hyperconjugative $\pi \rightarrow \sigma^*_{C-O}$ interactions (Table 1). Thus, the difference between **1** and **2–3** was due to the remote steric strain in the starting materials, which implied both the destabilization of the starting materials (enthalpic effect, *i.e.*,

decrease in E_a) and a better conformation of the aromatic ring at the reactive center (reduction in activation entropic cost), and the relief of this remote steric strain at TS which involved more freedom for the motions at TS (activation entropic effect, *i.e.*, $\Delta S^\ddagger > 0$) for **2** and **3** than for **1**. This takes into account the two-fold increase in k_d from **1** to **2** but not the two-fold increase from **2** to **3**.

As the homolysis of **2** and **3** afforded either the same radicals or its enantiomer, the difference in k_d was not due to the stabilization of the products. Amazingly, calculations showed that the faster isomer **3** was more stable than **2** by 3.0 kJ/mol, as highlighted by the $d_{\text{H}_{12}\cdots\text{C}_{10}}$. Consequently, the difference was due to the destabilization of TS. As highlighted by the 0.02 Å shorter $\text{C}_{18}\cdots\text{H}_{12}$ distance in **2** than the $\text{C}_1\cdots\text{H}_{12}$ distance in **3**, the phenyl ring induced larger steric strain than the methyl group [30], which in turn indirectly constrained the reaction center, as mentioned above (smaller $d_{\text{H}_{12}\cdots\text{C}_{10}}$ for **2** and **3** than for **1**). Thus, the *anti* conformation for the aromatic rings in **3** was more stable than the *gauche* conformation for the aromatic rings in **2** (Figure 5).

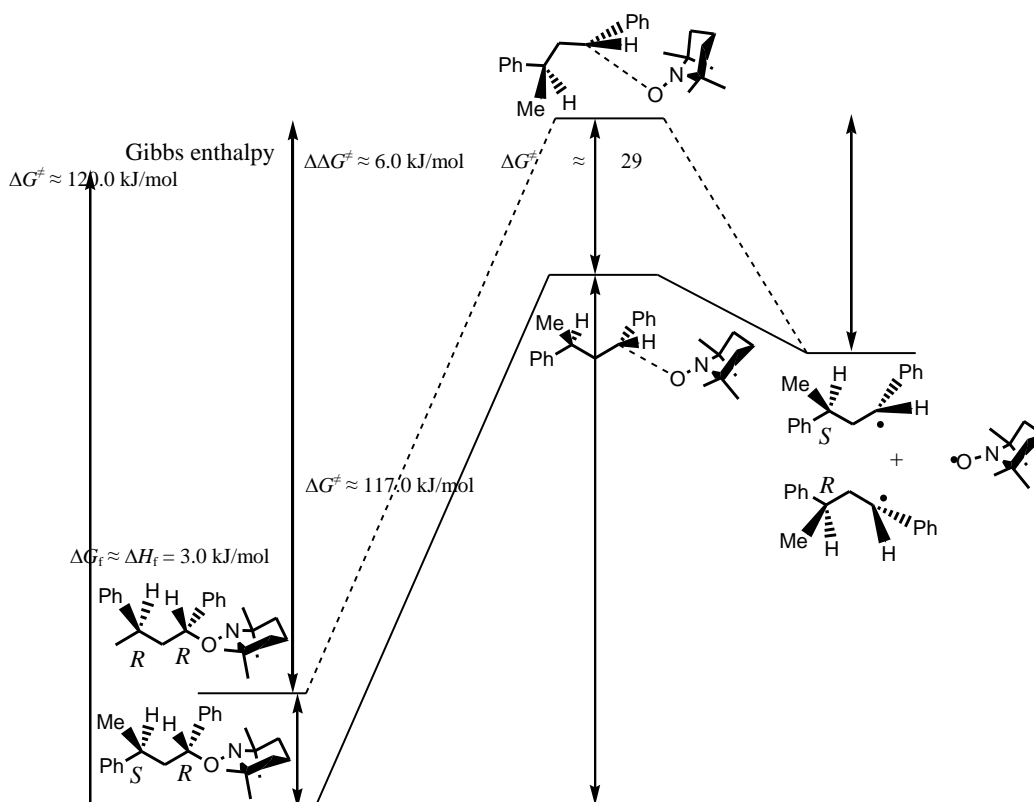
Figure 5. Conformations for the alkyl fragment 2–4.



As mentioned above, diastereoisomers **2** and **3** afforded a pair of enantiomeric radicals, and as their TS were product-like, the same interactions as those observed in the radicals and consequently their conformations should be observed in their respective TS [29]. As molecules were large and afford many conformations, and as energy changes were small, only the conformation [31] and the subsequent hyperconjugative interactions in starting materials were investigated by calculations. The weak 2 electron—2 orbital interactions mentioned above for **4** combined to the steric strain led to a preferred conformation exhibiting a W arrangement for the $\text{C}_{18}\text{C}_2\text{C}_3\text{C}_4\text{SOMO}$ bond/orbital sequence ($\langle\text{C}_1\text{C}_2\text{C}_3\text{C}_4\rangle \approx 61^\circ$ in Table 1 and Figure 4b) and, thus, such conformation was expected to occur at TS. Interestingly, the faster diastereoisomer **3** exhibited this W arrangement ($\langle\text{C}_1\text{C}_2\text{C}_3\text{C}_4\rangle \approx 63^\circ$, Figures 3g and h) whereas diastereoisomer **2** ($\langle\text{C}_1\text{C}_2\text{C}_3\text{C}_4\rangle \approx 173^\circ$, Figures 2e and f) did not. It should be mentioned that the weak $n_{\sigma,\text{O}} \rightarrow \sigma^*_{\text{C}_3-\text{C}_4} / \sigma_{\text{C}_3-\text{C}_4} \rightarrow \pi^*_{\text{C}_{18}}$ interactions (Table 1) supported that the W conformation for **3** was mainly due to the steric strain of the phenyl and methyl groups although the less tilted phenyl group ($\langle\text{C}_{19}\text{C}_{18}\text{C}_2\text{C}_3\rangle = 67^\circ$) afforded a slightly better interaction for **3** than for **2**. Consequently, as the alkyl fragment of **3** and the alkyl radical exhibited the same conformation—except at the C_4 center whose hybridization changed from sp^3 to sp^2 —no entropic cost was associated

with reaching TS from **3**. On the other hand, the alkyl fragment of **2** exhibited a conformation quite different from that of **5**, and consequently, reaching the expected conformation or a close one at TS required at least one C₂–C₃ bond rotation, leading to a highly sterically strained conformer, and more likely several bond rotations, leading to high entropic cost. Thus, although **3** was more stabilized than **2**, the lower entropic cost associated with reaching TS from **3** than from **2** afforded a faster cleavage for **3** than for **2** ($\Delta G^\ddagger(\mathbf{3}) < \Delta G^\ddagger(\mathbf{2})$), as depicted in Figure 6.

Figure 6. Pathways and expected TS [32] for the homolysis of **2** and **3** [33].



The Arrhenius parameters reported for the diastereoisomers of **7** ($A = 3.1 \times 10^{15} \text{ s}^{-1}$ and $E_a = 139.2$ kJ/mol for the *RR/SS* isomer, and $A = 5.5 \times 10^{14} \text{ s}^{-1}$ and $E_a = 131.2$ kJ/mol for the *RS/SR* isomer) deserve some comments assuming that the size, the conformation, and the polarity of the PhCOO group have very minor effects on the latter [34]. Internal strains in **2/3** (and, hence, in **7**) are larger than in **1**, implying the destabilization of **2/3** (and **7**). However, as the alkyl radical released by **2/3** (and **7**) is less stabilized than the one from **1**, TS for **2/3** (and **7**) is slightly higher in energy, which balances the energetic gain due to the destabilization of the starting material. Consequently, E_a for the isomers of **7** should be very close to E_a of **1** as observed for the *RS/SR* isomer. Thus, the change of k_d should be mainly observed by a change of A values. TS for **2** is more hindered than TS for **3**, thus, it costs activation entropy to be reached. Consequently, a higher A value is expected for the *RS/SR* isomer of **7** than for its *SS/RR* isomer, in sharp contrast to the reported values, although the A value for the *RS/SR* isomer is in the expected range. In fact, this clear difference observed between expectations from calculations and the experimental values is only due to the compensation entropy-activation energy [7].

4. Conclusion

As a conclusion, the increase in k_d in the series $1 < 2 < 3$ was due to a remote steric effect which induced enthalpic (destabilization of the starting materials and relief of steric strain at TS) and entropic (increase in freedom of motion and reduction in entropic costs both at TS) effects. Interestingly, this remote polar effect did not change the typical geometric parameters at the C–ON bond moiety. Importantly, the conclusions drawn here cannot be straightforwardly extended to alkoxyamines carrying a chiral nitroxide fragment such as TIPNO and SG1 because chirality close to the C–O–N moiety is expected to modify more or less strikingly the conformation, leading to an unexpected effect on k_d , as already reported [35].

X-ray of **1** and structures of **1–5** are provided as Cif, pdb, and mol2 files in supplementary materials.

References and Notes

1. Solomon, D.H.; Rizzardo, E; Cacioli, P. Polymerization process and polymers produced thereby. U.S. Patent 4,581,429, 11 July 1984.
2. Braunecker, W.A.; Matyjaszewski, K. Controlled/living radical polymerization: Features, developments, and perspectives. *Prog. Polym. Sci.* **2007**, *32*, 93–146.
3. Goto, A.; Fukuda, T. Kinetics of living radical polymerization. *Progr. Polym. Sci.* **2004**, *29*, 329, and references cited therein.
4. Fischer, H. The persistent radical effect: A principle for selective radical reactions and living radical polymerizations. *Chem. Rev.* **2001**, *101*, 3581, and references cited therein.
5. Fischer, H.; Souaille, M. The persistent radical effect in living radical polymerization—Borderline cases and side reactions. *Chimia* **2001**, *55*, 109–113.
6. Hawker, C.J.; Bosman, A.W.; Harth, E. New polymer synthesis by nitroxide mediated living radical polymerizations. *Chem. Rev.* **2001**, *101*, 3661–3688.
7. Bertin, D.; Gigmes, D.; Marque, S.R.A. Trialkylhydroxylamines (Alkoxyamines) in Radical Chemistry: Preparation, Stability and Applications. *Recent Res. Devel. Org. Chem.* **2006**, *10*, 63–121.
8. Chauvin, F.; Dufils, P.E.; Gigmes, D.; Guillaneuf, Y.; Marque, S.R.A.; Tordo, P.; Bertin, D. Nitroxide-mediated polymerization: The pivotal role of the $k(d)$ value of the initiating alkoxyamine and the importance of the experimental conditions. *Macromolecules* **2006**, *39*, 5238–5250.
9. Bagryanskaya, E.; Bertin, D.; Gigmes, D.; Kirilyuk, I.; Marque, S.R.A.; Reznikov, V.; Roshchupkina, G.; Zhurko, I.; Zubenko, D. Can the first addition of alkyl radicals play a role in the fate of NMP? *Macromol. Chem. Phys.* **2008**, *209*, 1345–1357.
10. Bertin, D.; Dufils, P.-E.; Durand, I.; Gigmes, D.; Giovanetti, B.; Guillaneuf, Y.; Marque, S.R.A.; Phan, T.; Tordo, P. Effect of the penultimate unit on the C–ON bond homolysis in SGi-based alkoxyamines. *Macromol. Chem. Phys.* **2008**, *209*, 220–224.
11. Nicolas, J.; Dire, C.; Mueller, L.; Bellenev, J.; Charleux, B.; Marque, S.R.A.; Bertin, D.; Magnet, S.; Couvreur, L. Living character of polymer chains prepared via nitroxide-mediated controlled free-radical polymerization of methyl methacrylate in the presence of a small amount of styrene at low temperature. *Macromolecules* **2006**, *39*, 8274–8282.

12. Guillaneuf, Y.; Gigmes, D.; Marque, S.R.A.; Tordo, P.; Bertin, D. Nitroxide-mediated polymerization of methyl methacrylate using an SG1-based alkoxyamine: How the penultimate effect could lead to uncontrolled and unliving polymerization. *Macromol. Chem. Phys.* **2006**, *207*, 1278–1288.
13. Li, L.C.; Hamer, G.K.; Georges, M.K. A quantitative H-1 NMR method for the determination of alkoxyamine dissociation rate constants in stable free radical polymerization. Application to styrene dimer alkoxyamines. *Macromolecules* **2006**, *39*, 9201–9207.
14. Configuration and conformation of the *S,S* diastereoisomer was determined by X-ray analysis. See Reference 13.
15. Bon, S.A.F.; Chambard, G.; German, A.L. Nitroxide-mediated living radical polymerization: Determination of the rate coefficient for alkoxyamine C–O bond homolysis by quantitative ESR. *Macromolecules* **1999**, *32*, 8269.
16. Goto, A.; Fukuda, T. Kinetic study on nitroxide-mediated free radical polymerization of tert-butyl acrylate. *Macromolecules* **1999**, *32*, 618–623.
17. Guillaneuf, Y.; Gigmes, D.; Marque, S.R.A.; Tordo, P.; Bertin, D. First effective nitroxide-mediated polymerization of methyl methacrylate. *Macromolecules* **2007**, *40*, 3108–3114.
18. Edeleva, M.V.; Kirilyuk, I.A.; Zubenko, D.P.; Zhurko, I.F.; Marque, S.R.A.; Gigmes, D.; Guillaneuf, Y.; Bagryanskaya, E.G. Kinetic Study of H-atom Transfers in Imidazoline-, Imidazolidine-, and Pyrrolidine-Based Alkoxyamines: Consequences for Nitroxide Mediated Polymerization. *J. Polym. Sci. Polym. Chem. A* **2009**, *47*, 6579–6595.
19. Beaudoin, E.; Bertin, D.; Gigmes, D.; Marque, S.R.A.; Siri, D.; Tordo, P. Alkoxyamine C–ON bond homolysis: Stereoelectronic effects. *Eur. J. Org. Chem.* **2006**, *7*, 1755–1768.
20. Bertin, D.; Gigmes, D.; Marque, S.R.A.; Siri, D.; Tordo, P.; Trappo, G. Effect of the carboxylate salt on the C–ON bond homolysis of SG1-based alkoxyamines. *Chem. Phys. Chem.* **2008**, *9*, 272–281.
21. Marque, S.R.A.; Siri, D. Is Experimental Evidence Sufficient Enough To Account for the Stabilization Effect of Bisnitroxide on the Fate of NMP Experiments? *Macromolecules* **2009**, *42*, 1404–1406.
22. Frisch, M.J.; Trucks, G.W.; Schlegel, H.B.; Scuseria, G.E.; Robb, M.A.; Cheeseman, J.R.; Montgomery, J.A., Jr.; Vreven, T.; Kudin, K.N.; Burant, J.C.; *etc.* *Software for calculations: Gaussian 03*, Revision C.02. Gaussian, Inc.: Wallingford, CT, USA, 2004. Available online: <http://www.gaussian.com> (accessed on 21 September 2010).
23. It is well known that geometry optimization performed by DFT with the B3LYP method provides geometries as reliable as those obtained with the *ab initio* MP2 methods. See: Koch, W.; Holthausen, M.C. *A Chemist's Guide to DFT*, 2nd ed.; Wiley-VCH: Weinheim, Germany, 2001; Chapter 8, pp. 119–136.
24. Calculations were started from conformations different from those displayed in Figures 1 and 2. In each case, conformations displayed in Figures 1 and 2 appeared as the most stable.
25. The B3P86 method was chosen to calculate energies because it is known to provide the most accurate values. See: Feng, Y.; Liu, L.; Wang, J.-T.; Huang, H.; Guo, Q.-X. Assessment of Experimental Bond Dissociation Energies Using Composite *ab Initio* Methods and Evaluation of

- the Performances of Density Functional Methods in the Calculations of Bond Dissociation Energies. *J. Chem. Inf. Comput. Sci.* **2003**, *4*, 2005–2013.
26. Reed, A.E.; Curtiss, L.A.; Weinhold, F.A. Intermolecular Interactions from a Natural Bond Orbital, Donor-Acceptor Viewpoint. *Chem. Rev.* **1988**, *88*, 899–926.
 27. Moad, G.; Rizzardo, E. Alkoxyamine-initiated living radical polymerization: Factors affecting alkoxyamine homolysis rates. *Macromolecules* **1995**, *28*, 8722–8728.
 28. Lagrille, O.; Cameron, N.R.; Lovell, P.A.; Blanchard, R.; Goeta, A.E.; Koch, R. Novel acyclic nitroxides for nitroxide-mediated polymerization: Kinetic, electron paramagnetic resonance spectroscopic, X-ray diffraction, and molecular modeling investigations. *J. Polym. Sci. Polym. Chem.* **2006**, *44*, 1926–1940.
 29. TS involving large molecules and conformational changes are time-consuming and often difficult to determine, especially when the difference between TS is expected to be small. Thus, we preferred to discuss our results applying the Hammond postulate.
 30. At first glance, it was not obvious that the phenyl group was bulkier than the methyl group because it is known as a Janus group whose size can be much smaller or much larger than that of the methyl group.
 31. The conformation calculated for the enantiomer *RR* of **2** correspond to the conformation reported for the *SS* enantiomer of **7** [13]. It was assumed that the conformation given by the X-ray data was the most stable.
 32. As TS were not calculated [29], the activation barriers ΔG^\ddagger were estimated with the Arrhenius parameters reported in [13]. As the cross-coupling rate constants to yield the unimeric ($k_c = 2.2 \times 10^8 \text{ l mol}^{-1} \text{ s}^{-1}$) and polymeric ($k_c = 1.8 \times 10^8 \text{ l mol}^{-1} \text{ s}^{-1}$) species at 20 °C were very close (Guillaneuf, Y.; Bertin, D.; Castignolles, P.; Charleux, B. New experimental procedure to determine the recombination rate constants between nitroxides and macroradicals. *Macromolecules* **2005**, *38*, 4638–4646), ΔG^\ddagger for **2** and **3** to reach TS from the products were likely very close to the one reported for the formation of **1** ($\Delta G^\ddagger = 28.6 \text{ kJ mol}^{-1}$, $A = 4.0 \times 10^{11} \text{ l mol}^{-1} \text{ s}^{-1}$, $E_a = 15.5 \text{ kJ mol}^{-1}$, Sobek, J.; Martschke, R.; Fischer, H. Entropy control of the cross-reaction between carbon-centered and nitroxide radicals. *J. Am. Chem. Soc.* **2001**, *123*, 2849–2857).
 33. It was assumed that the contribution of the entropic term to the total energy of the molecule was negligible to the enthalpic term, and thus, $\Delta G_f \approx \Delta H_f$
 34. Although PhCOO group is larger than H atom it should not generate larger strain than the methyl group of the model **2/3** due to its conformation in the same plane than the backbone as given by the X-ray structure (see Reference 13). The effect of the polarity of PhCOO group ($\sigma_{\text{I,AcOCH}_2} = 0.15$) on the reactive center is buffered by the sequence $\text{CH}_2\text{CPhHCH}_2$.
 35. Marque, S.; Le Mercier, C.; Tordo, P.; Fischer, H. Factors influencing the C–O– bond homolysis of trialkylhydroxylamines. *Macromolecules* **2000**, *33*, 4403–4410.